NIPES

Journal of Science and Technology Research

Journal homepage: www.nipesjournals.org.ng

Residual Stress Optimization in Mild Steel Welded Joint using Finite Element Method

Eboigbe[a], C.I., Achebo[b], J.

[a,b]Dept. of Production Engineering, University of Benin, Edo state, Nigeria

E-mail : kristoeboi@gmail.com

ARTICLE INFORMATION

Article history:
Received 27 February 2019
Revised 10 March 2019
Accepted 15 March 2019
Available online 25 March 2019

Keywords:
Central Composite design
FEM
ANSYS
Optimization
Residual Stress
TIG welding

ABSTRACT

Residual stress has detrimental effect on the quality, reliability and service life of welded joints. Tungsten Inert Gas (TIG) welding is a very popular gas shielding arc welding process used in many industrial fields. Welded joints produced as a result of poor combination of process parameters do not possess sufficient strength required to sustain its useful service life. This study was carried out with the aim of optimizing residual stress in mild steel weldment using Finite Element Method (FEM). In order to address the problem of residual stresses, the finite element method was employed. The experimental matrix was made of thirty (30) runs, generated by the design expert 7.01 software adopting the central composite design. The parameters considered in this study were current, voltage, gas flow rate and welding speed. The material used was 80mm x 60mm x 6mm mild steel plates. The response was measured using the ultrasonic computerized complex and the finite element analysis of residual stresses in Butt welding of the two similar plates was performed with the ANSYS software. In this study, the FEM was employed to optimize the residual stresses in the mild steel welded joints. This study has shown that current, gas flow rate, welding speed and voltage had a very strong influence on residual stress formation. The model produced numerical optimal solution of current 180 Amp, voltage of 16volt, welding speed of 351mm/min and gas flow rate of 16Lit/min, which will produce a welded material having a residual stress of 265MPa.

1. Introduction

Our safety and peace of mind is heavily dependent on our capacity to prevent, predict and postpone the failure of engineering structures and components [1]. Welding process relies on an intensely localized heat input, which tends to generate undesired residual stresses and deformations in welded structures, especially in the case of thin plates. The advantages of welding as a joining process include high joint efficiency, simple set up, flexibility and low fabrication costs. However when structures are manufactured by welding, a non-uniform temperature distribution is produced. This distribution initially causes a rapid thermal expansion followed by a thermal contraction in the weld and surrounding areas, thus generating inhomogeneous plastic deformation and residual stresses in the weldment when it is cooled [2].

Residual stresses in structural materials or components are those stresses which exist in the object without the application of any service or other external loads [3]. Residual stress is an unavoidable concomitant of almost all manufacturing and fabrication processes and can also arise during service; they will occur under any set of circumstances that lead to differential expansion or contraction

between adjacent parts of a body in which the local yield strength is exceeded [4]. Virtually all manufacturing processes e.g. casting, welding, machining, forging, e.t.c introduce residual stresses into the manufactured object [5]. Distribution of residual stresses in welded joints are strongly affected by structural parameters (geometry and joint type), material parameters (mechanical and physical properties), and welding process parameters such as current, voltage, gas flow rate, welding speed, e.t.c [6,7,8,9]. Quenching treatments produce residual stresses, while stress-relieving heat treatments may reduce such stresses. Heat from welding may cause localized expansion, which is taken up during welding by either the molten metal or the placement of parts being welded. The main cause of residual stress formation is inhomogeneous deformation. The processes involving high temperatures often lead to residual stresses as different regions cool at different rates causing inhomogenous deformation. Localised heating by the welding arc and the subsequent rapid cooling leads to the formation of residual stresses in weldments. The magnitude of residual stress in regions near the weld can be as high as the yield strength of the material being welded. In heat treatment of metals, if it is cooled rapidly, the surface and the interior contract at different rates. The surface regions, because of the temperature gradient, contract more than the interior. By the time the interior begins to cool, the outer regions are already rigid, resulting in compressive stresses at the surface balanced by tensile stresses in the interior. However, if the material undergoes phase transformation with volume changes, the state of stress gets altered. In some cases tensile residual stresses are observed.

Residual stresses locked in during manufacturing processes are often detrimental to the integrity and service behaviour of components. High tensile residual stresses in areas near the weld cause fracture under certain condition. Many efforts are made to predict and relax residual stresses in welded structures. A well-known method of stress relieving is by heat treatment. Other equally effective methods of stress relief are typically mechanical. These include localised peening, shot blasting, hydrostatic testing and vibratory stress relieving [10]. Relevant advances in numerical and experimental stress relieving techniques should be explored to provide protection against the risk of initiation and propagation of brittle fracture [11]. The aim of this study is to optimize residual stress in mild steel welded joint using the Finite Element Method.

2. Materials and Method

Mild steel plate of thickness 6 mm was selected as material used for the experiment. The mild steel plate was cut to dimension of 80 mm x 60 mm with the help of power hacksaw and grinded at the edge to smoothen the surfaces to be joined. In this experiment the butt weld joint made of two similar mild steel plates was employed. The surfaces of the coupon were polished with emery paper, thereafter the mild steel plates were fixed on the work table with flexible clamp to weld the joints of the specimen. A TIG welding process was used with Alternate Current (AC) to perform the experiments as it concentrates the heat in the welding area, using 100% argon gas as the shielding gas, residual strain was measured for each sample using ultrasonic technique. For each experimental runs 5 specimens were used, and the average of the 5 experimental readings was recorded each for the 30 runs. The two mild steel plates were arranged and the temperature was measured using K-type thermocouple which was connected to the digital thermometer. The thermocouple were attached to the plate at different distances. The values of the current and voltage were set on the welding machine and the gas flow rate was adjusted. The stop watch was used to measure the duration of the welding process. Using the time and distance travelled by the electrode during the welding process, the welding speed was calculated.

The welding parameters used in this study were current 180amp, voltage 16volts, gas flow rate 18.04 Lit/min, welding speed 351mm/min.

The amount of heat input during welding, Q was calculated as follows:

$$\text{Heat input rate } (Q) = V \times I \times 60/U \text{ (J/mm)} \quad (1)$$

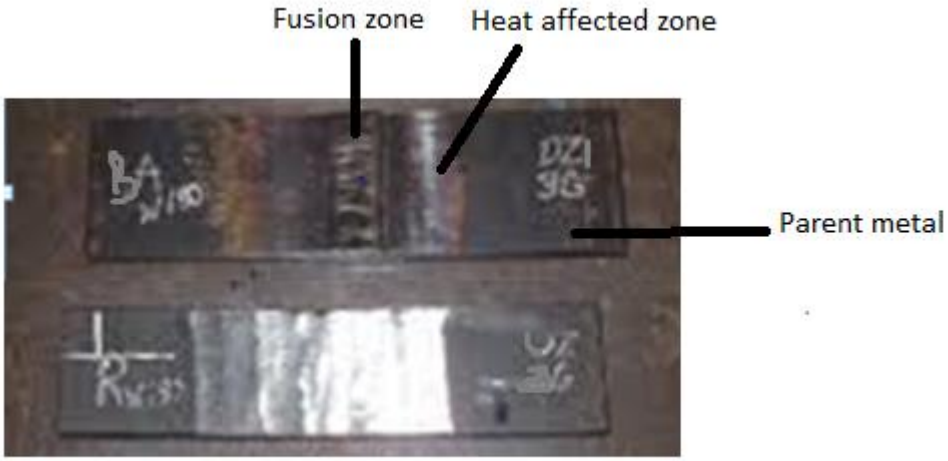

Figure 1: Experimental Samples

2.1. Temperature distribution in welded plate using FEM

Mild steel was used for this simulation and the thermo-mechanical property is reported in Table 1.

Table 1: Material Properties of Mild Steel

Temperature (°C)	Density (kg m^-3)	Coefficient of Thermal Expansion (C^-1)	Young's Modulus (Pa)	Poisson's Ratio	Thermal Conductivity (W m^-1 C^-1)
0	7880	1.15	2.1E+11	0.3	60
100	7880	1.2	2E+11	0.3	50
200	7880	1.3	2E+11	0.3	45
400	7760	1.42	1.7E+11	0.3	38
600	7600	1.45	80000000000	0.3	30
800	7520	1.45	35000000000	0.3	25
1000	7390	1.45	20000000000	0.3	26
1200	7300	1.45	15000000000	0.3	28
1400	7250	1.45	10000000000	0.3	37
1550	7180	1.45	10000000000	0.3	37

2.2. Analysis and Proceedure

The commercial finite element software (ANSYS) was used for the simulation. The procedure started with modeling the geometry of the welded sampled as shown in Figure 2. The sample was dimensionally specified as 80mm X 60mm X 6mm. The standard trapezoidal mesh element of size 5mm was used to discretize the geometry. This is shown in Figure 3.

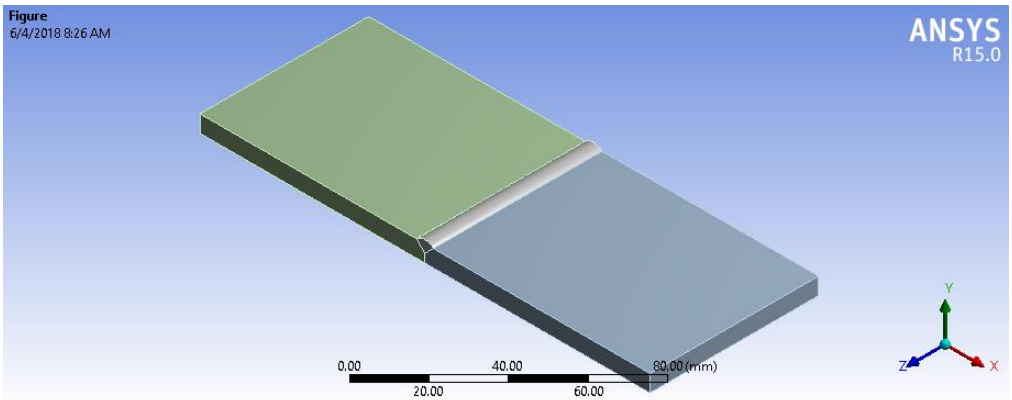

Figure 2: 3D CAD Model of Closed Butt-weld Joint Geometry of Welded Sample

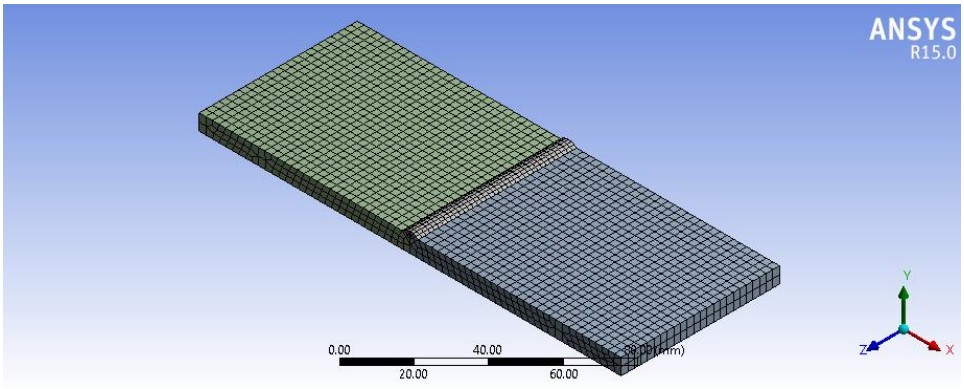

Figure 3: Finite Element Discretization of the Geometry

The governing equations for the material model undergoing phase transformation during welding is given as:

$$c(t) = m\left[1 - \cos 2\pi\left(\frac{T - T_s}{T_l - T_s}\right)\right] T_s < T < T_l \tag{2}$$

Welding is indicated by the history variable given as:

$$\gamma(t) = min\left(1, \left(max_{s\leq t}\gamma(s), \frac{T - T_l^{start}}{T_l^{end} - T_l^{start}}\right)\right) \tag{3}$$

The effective thermal material properties are interpolated as

$$\widetilde{c_p} = c_p(T)\gamma + c_p^{quiet}(1-\gamma) \tag{4}$$

$$\tilde{\mu} = \mu(T)\gamma + \mu^{quiet}(1-\gamma) \tag{5}$$

where c_p and μ are the heat capacity and thermal conductivity, respectively.

The residual stress in the material is given by [12] as:

$$\sigma_y = (A + B\bar{\varepsilon}^{pn})(1 + c\ln\dot{\varepsilon}^*)(1 - T^{*m}) \tag{6}$$

The thermal distribution within the welded samples $T(x, y, z)$, where x, y, z are the three coordinate distances, is governed by the following one-dimensional partial differential equation:

$$\rho C\frac{\partial T}{\partial \tau} = \frac{\partial}{\partial x}\left(k\frac{\partial T}{\partial x}\right) \tag{7}$$

Where τ is the characteristic response time of the material which property k is taken as a variable, and

ρ and C are the material density and specific heat respectively.

For convective cooling of the samples, the energy equation is written for as given below:

$$\rho C_p\left(\frac{\partial T}{\partial \tau} + u\frac{\partial T}{\partial x} + v\frac{\partial T}{\partial x}\right) = \frac{\partial}{\partial x}\left(k\frac{\partial T}{\partial x}\right) + \frac{\partial}{\partial y}\left(k\frac{\partial T}{\partial y}\right) \tag{8}$$

where C_p is the specific heat of the ambient air at constant pressure, and u and v are the velocity components in the x and y directions, respectively.

2.3. Optimization

The simulation input variables were used to perform a direct optimization using Multi-Objective Genetic Algorithm (MOGA) method. The method generates 50 initial samples and 25 samples per iteration from the input variables to form the design points and calculates the responses at each point. The maximum allowable Pareto percentage was set at 70 per cent. Three best candidates from the design points which yield the optimum responses were then selected. The optimization simulation converged after 5 iterations and generated 150 optimization data.

3. Results and Discussion

The result of the simulation is presented Figures 4-6.

3.1. Steady State Temperature Distribution

Figure 4 shows the steady state temperature distribution of the welded sample. The maximum temperature corresponding to the solidus temperature is recorded as 1557.8^{o}C at the heat affected zone (HAZ). Away from the HAZ, the temperature is recorded as reducing until a minimum value of 22^{o}C corresponding to the ambient temperature is reached.

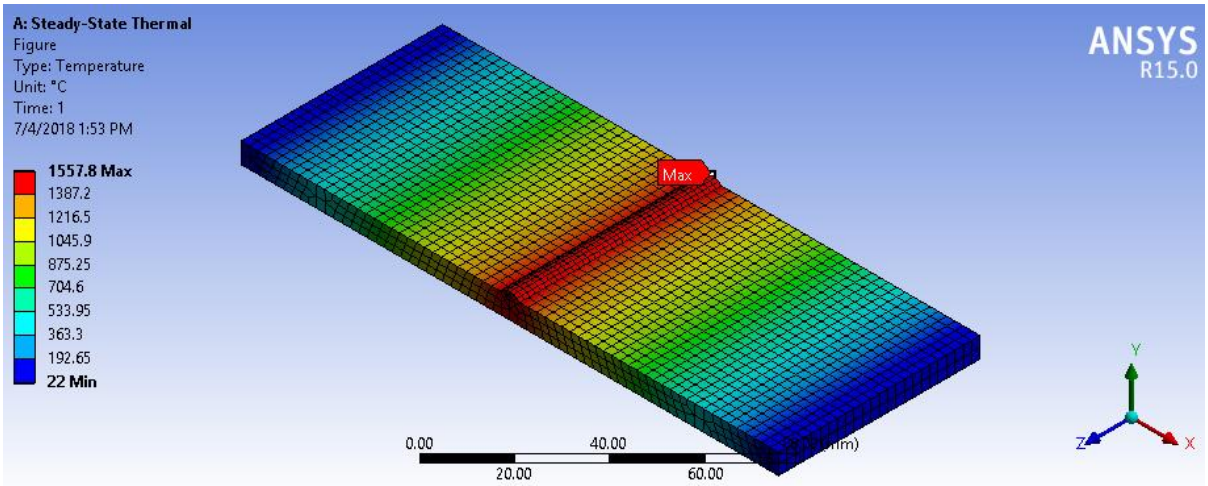

Figure 4: Steady State Temperature Distribution

3.2 Residual Stress Distribution

Figures 5 and 6 show the distribution of residual stresses on the welded sample. Under the simulation condition the maximum residual stress is recorded as 294.19MPa. The maximum stress value is located at the edge of the HAZ as can readily be seen from Figure 5.

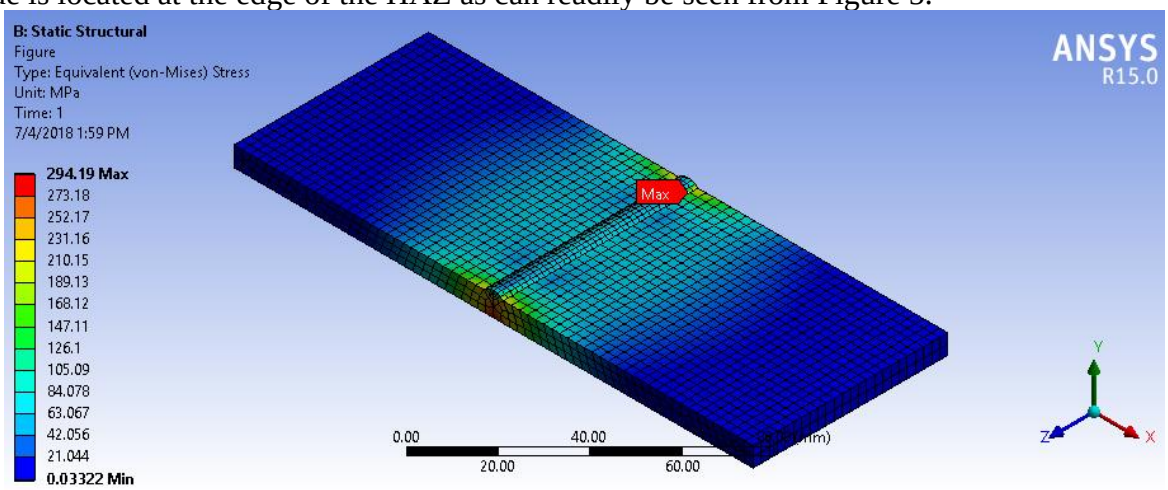

Figure 5: Residual Stress Distribution (Equivalent von Mises)

The stress distribution is captured as wave represented by isolines in Figure 6. The isolines map out the region of different stress values in the welded sample. It is easy to see with the aid of the isolines that the maximum residual stress is localized to the edge of the welded sample.

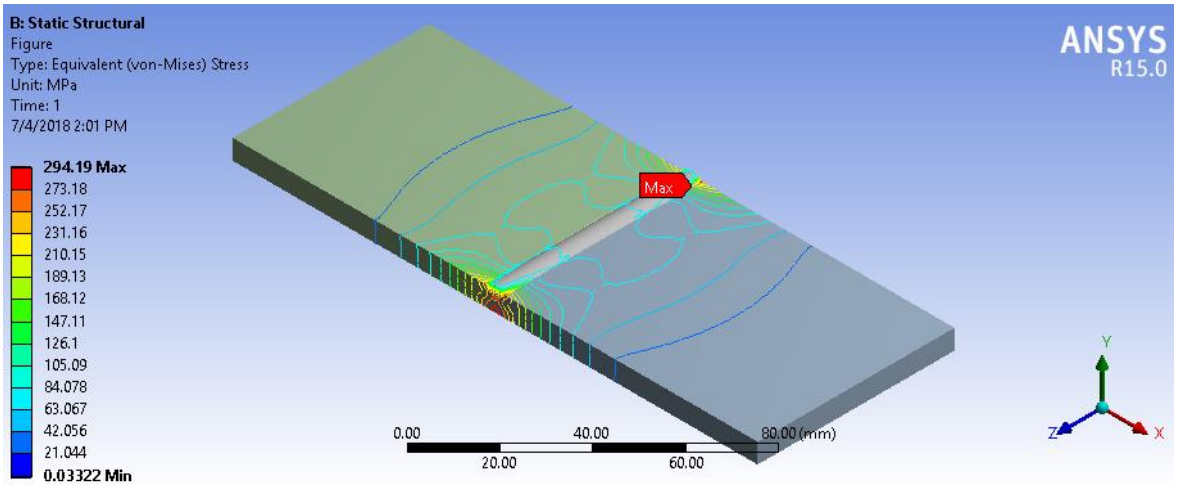

Figure 6: Residual Stress Distribution as Stress Wave on Welded Geometry

The residual stress obtained in this study is however, relatively low as compared to values obtained by Nuraini et.al and Rakesh [13, 14]. This can be attributed to proper selection of process parameters (current, voltage, welding speed and gas flow rate), welding process employed and smaller size of welding plate.

3.3. Optimum Responses

The raw data of design points or pareto fronts generated from the optimization is shown in Table A1 (Appendix A). The optimization result from the generated design points using the screening method is shown in Table 2.

Table 2: Optimal Solutions of Numerical Optimization

S/N	Current (Amp)	Voltage (volt)	Gas Flow Rate (lit/min)	Welding Speed (mm/min)	Equivalent Stress Maximum (MPa)
1	180.00	18.00	16.00	351.00	265.0000

4. Conclusion

The integrity of a weld is determined by the geometry, joint type and optimal combination of process parameters. For optimization of the welding parameters, different combinations of the current, voltage, gas flow rate and welding speed were used. If the values of the current, gas flow rate, welding speed and voltage are increased, the residual stresses also increases. From the results of Table 3, it can be deduced that the optimum welding parameters for the weldability of mild steel weld specimen of dimension 80mm× 60mm × 6 mm for minimum residual stress of 265MPa were current 180amp, voltage 18.00volt, gas flow rate 18.04lit/min and welding speed 351mm/min. In this study, the finite element method was used to optimise residual stress present in welded mild steel plates. The optimum results obtained can help to produce weld pool with fewer spatters, less defects and a favourable kinematic viscosity which translates into a high quality weldment [15]. It has been shown that the optimization and prediction of residual stress can improve the reliability, service life and integrity of welded joints. It is therefore recommended that welding and fabrication industries should endeavour to use the optimum welding process parameters achieved in this study to produce high quality welds in Tungsten inert gas welding process.

Nomenclature

V	*Voltage (volt)*
I	*Current (Ampere)*
U	*Welding speed (mm/min)*
T_l	*Liquidus temperature (°C)*
T_s	*Solidus temperature (°C)*
T	*Welding temperature, (°C)*
m	*Multiplier such that* $\lambda = \int_{T_s}^{T_l} c(T)dT$
λ	*Latent heat (Joule)*
c	*Heat capacity (J/kg^{-1}°C)*
A	*Yield strength (MPa)*
B	*Hardening modulus (MPa)*
n	*Thermal softening coefficient*
m	*Hardening coefficient*
$\bar{\varepsilon}^p$	*Effective plastic strain, mm*
T^*	*Homologous temperature* $= \frac{T-T_{ambient}}{T_l-T_{ambient}}$
$\dot{\varepsilon}^*$	*Effective total strain rate, mm*

5. Conflict of Interest

There is no conflict of interest associated with this work.

References

[1] Withers, P.J., Turski, M, Edwards, L,. Bouchard, P.J. and Buttle, D.J (2008). Recent advances in residual stress measurement. International Jounal of Presssure Vessels and Piping. 85(3): 118-127.

[2] Armentani,E, Esposito, R and. Sepe, R. (2007). The effect of thermal properties and weld efficiency on residual stresses in welding. Journal of Achievements in Materials and Manufacturing Engineering, 20(I1-2): 319-322.

[3] Withers, P.J.(2007). Residual stress and its role in failure. (2007). Reports on progress in physics, vol.70, pp 2211-2264.

[4] Chinnaraj,K Sathya, P.M, Lakshmana. R,C. (2013). Numerical and experimental investigation of residual stresses in cold formed truck frame rail sections, SAE Technical paper.

[5] Withers, P. J. and Bhadeshia, H. K. D. H (2001). Residual stress Part 2 – Nature and origins – Overview. Materials Sci .and Tech.,, Vol. 17, pp. 366-375.

[6] Celestino, V,. Loureiro,A .Pina, J, and. Batista, A.C (2002). Residual stress distribution in butt welded joints- Effect of the weld Groove shape. Materials Science. Vol. 404, pp.387-392.

[7] Jeyakumar, M., Christopher,T, Narayanan, R and Nageswara Rao, B (2011) Residual stress evaluation in butt-welded steel plates. Indian Journal of Engineering and Materials Sciences, Vol. 18,pp. 425-434.

[8] Wei ,L Hidekazu, M and Dean, D (2015). Investigation of welding residual stress distribution in a thick-plate joint with emphasis on the features near weld end-start. Materials and Design.Vol.67, pp. 303-312.

[9] Feng, Z., Wang, X.L., David, S.A., and Sklad, P.S.(2007).Modelling of residual stresses and property distributions in friction stir welds of Aluminum alloy 6061-T6. Science and Technology of welding and joining.Vol 12, pp. 348-356.

[10] Hornsey,J, S (2006). Residual Stresses: Their causes and the effective means of Treatment to reduce the residual stresses and to improve the fatigue life in Engineering components.. J.S Hornsey of vibratory stress Relieving, Leraatsfontein, South Africa.

[11] Coules, H.E. (2012).Contemporary approaches to reducing weld induced residual stress. Materials Science and Technology. Vol. 29, pp.4-18.

[12] Johnson, G., Cook, W. A (1983). Constitutive Model and Data for Metals Subjected to Large Strains, High Strain Rates and High Temperatures. In Proceedings of the 7th International Symposium on Ballistics, The Hague, The Netherlands, Vol.1, pp. 541–547.
[13] Nuraini, A.A., Zainal, A.S.M and Azmah, M.A. (2013). The Effect of Welding Process Parameter on Temperature and Residual Stress in Butt-Joint weld of Robotic Gas Metal Arc Welding. Australian Journal of Basic and Applied Sciences. Vol. 7, pp. 814-820.
[14] Rakesh, K and Guriurinder, S.B. (2017). Optimization of Process Parameters for MIG Welding by Taguchi Method. International Journal of Scientific Research Engineering and Technology. Vol. 6, pp. 756-768.
[15] Joseph, A (2016). Experimental characterisation and numerical simulation of Fibre laser welding of AA 2024- T3 and Ti-6AI-4V. A Ph.D Thesis in the Department of Mechanical Engineering, Imperial College London.

Appendix A

Table A1: Raw Data of Design Points or Pareto Fronts

Design Points	Input Variables				Responses			
	Current (Amp)	Voltage (Volt)	Gas Flow Rate (Lit/min)	Welding Speed (mm/min)	Solidus Temperature (^oC)	Liquidus Temperature (^oC)	Safety Factor Minimum	Equivalent Stress Maximum (MPa)
1	180.40	18.00	16.00	351.00	1434.18	1453.20	0.94	265.00
2	181.20	20.08	19.37	371.00	1472.29	1479.61	0.93	269.89
3	182.00	18.08	20.71	391.00	1501.38	1525.04	0.911	274.41
4	182.80	22.08	18.48	411.00	1530.47	1570.47	0.90	278.94
5	183.60	17.08	19.82	431.00	1559.56	1615.89	0.88	283.46
6	184.40	21.08	21.15	355.00	1588.66	1661.32	0.87	287.99
7	185.20	19.08	18.93	375.00	1617.75	1706.75	0.85	292.52
8	186.00	23.08	20.26	395.00	1440.67	1646.84	0.84	297.04
9	186.80	16.58	21.60	415.00	1486.10	1675.93	0.83	301.57
10	187.60	20.58	18.19	435.00	1531.53	1705.02	0.82	306.09
11	188.40	18.58	19.52	359.00	1576.96	1734.11	0.80	310.62
12	189.20	22.58	20.85	379.00	1445.85	1622.38	0.79	315.15
13	190.00	17.58	18.63	399.00	1474.94	1667.81	0.78	319.67
14	190.80	21.58	19.97	419.00	1504.03	1713.24	0.94	265.71
15	191.60	19.58	21.30	439.00	1447.16	1533.12	0.93	270.23
16	192.40	23.58	19.08	363.00	1492.59	1562.21	0.91	274.76
17	193.20	16.33	20.41	383.00	1538.02	1591.30	0.90	279.29
18	194.00	20.33	21.74	403.00	1583.45	1620.39	0.88	283.81
19	194.80	18.33	18.34	423.00	1628.87	1649.48	0.87	288.34
20	195.60	22.33	19.67	443.00	1674.30	1678.57	0.85	292.86
21	196.40	17.33	21.00	367.00	1707.66	1719.73	0.84	297.39
22	197.20	21.33	18.78	387.00	1453.65	1736.75	0.83	301.92
23	198.00	19.33	20.11	407.00	1448.49	1499.08	0.82	306.44
24	198.80	23.33	21.45	427.00	1477.58	1544.51	0.80	310.97
25	199.60	16.83	19.23	447.00	1506.67	1589.94	0.79	315.49
26	200.40	20.83	20.56	351.80	1535.76	1635.36	0.78	320.02
27	201.20	18.83	21.89	371.80	1564.85	1680.79	0.94	266.06
28	202.00	22.83	18.09	391.80	1593.94	1726.22	0.92	270.58
29	202.80	17.83	19.42	411.80	1460.14	1623.04	0.91	275.11
30	203.60	21.83	20.76	431.80	1505.57	1652.13	0.89	279.63
31	204.4	19.83	18.53	355.80	155.10	1681.22	0.88	284.16
32	205.20	23.83	19.87	375.80	1596.43	1710.31	0.87	288.69
33	206.00	16.21	21.20	395.80	1641.85	1739.40	0.85	293.21
34	206.80	20.21	18.98	415.80	1451.13	1687.28	0.84	297.74
35	207.60	18.21	20.31	435.80	1480.23	1732.71	0.83	302.26
36	208.40	22.21	21.64	359.80	1466.63	1509.32	0.81	306.79
37	209.20	17.21	18.24	379.80	1512.06	1538.41	0.80	311.32
38	210.00	21.21	19.57	399.80	1557.49	1567.50	0.79	315.84
39	210.80	19.21	20.90	419.80	1596.59	1602.92	0.78	320.37
40	211.60	23.21	18.68	439.80	1625.68	1648.34	0.94	266.40
41	212.40	16.71	20.02	363.80	1654.77	1693.77	0.92	270.93
42	213.20	20.71	21.35	383.80	1683.86	1739.20	0.91	275.46
43	214.00	18.71	19.13	403.80	1473.12	1712.95	0.89	279.98
44	214.80	22.71	20.46	423.80	1518.55	1742.04	0.88	284.51

45	215.60	17.71	21.79	443.80	1453.78	1563.98	0.86	289.03
46	216.40	21.71	18.39	367.80	1482.87	1609.40	0.85	293.56
47	217.20	19.71	19.72	387.80	1511.96	1654.83	0.84	298.09
48	218.00	23.71	21.05	407.80	1541.05	1700.26	0.83	302.61
49	218.80	16.46	18.83	427.80	1570.14	1745.69	0.81	307.14
50	219.60	20.46	20.16	447.80	1435.11	1599.23	0.80	311.66
51	181.22	17.94	18.09	391.80	1493.28	1521.81	0.92	270.72
52	202.78	22.97	20.71	391.00	1602.05	1729.45	0.91	274.28
53	181.20	17.80	19.37	370.02	1460.98	1472.29	0.93	269.67
54	202.80	20.11	19.42	412.78	1478.76	1623.04	0.91	275.32
55	181.28	20.17	19.35	373.59	1504.03	1713.24	0.94	265.96
56	190.72	21.49	19.99	416.41	1472.29	1479.61	0.93	269.63
57	193.84	21.80	19.04	363.00	1492.59	1562.21	0.91	274.76
58	202.16	23.61	20.79	431.80	1505.57	1652.13	0.89	279.63
59	212.40	16.59	20.02	363.80	1654.77	1693.77	0.92	270.86
60	192.40	23.69	19.08	363.00	1492.59	1562.21	0.91	274.83
61	190.76	19.58	19.95	418.28	1447.16	1533.12	0.94	265.73
62	191.64	21.58	21.32	439.72	1504.03	1713.24	0.93	270.21
63	204.40	19.87	18.53	355.80	1551.00	1681.22	0.94	265.45
64	190.80	21.54	19.97	419.00	1504.03	1713.24	0.88	284.42
65	192.66	19.55	18.03	392.71	1488.67	1533.12	0.93	270.19
66	200.94	22.86	21.36	438.09	1593.94	1684.72	0.92	270.63
67	201.64	18.91	21.34	371.56	1555.83	1680.79	0.93	266.82
68	212.76	20.62	21.90	384.04	1692.89	1739.20	0.91	274.69
69	190.80	20.10	19.97	372.98	1504.03	1713.24	0.94	265.69
70	181.20	21.56	19.37	417.02	1472.29	1479.61	0.93	269.90
71	192.40	16.63	20.02	372.57	1446.21	1654.77	0.92	270.93
72	211.60	19.65	21.30	430.23	1533.12	1694.72	0.93	270.23
73	192.40	23.19	18.68	363.00	1488.86	1564.53	0.94	266.54
74	211.60	23.59	19.08	439.80	1623.35	1652.07	0.91	274.62
75	193.20	16.33	20.41	383.00	1538.02	1591.30	0.90	279.29
76	190.77	20.10	19.99	367.62	1504.03	1713.24	0.94	265.77
77	191.67	21.58	21.29	445.08	1504.03	1713.24	0.93	270.13
78	190.80	21.58	19.97	355.65	1517.34	1553.89	0.94	265.71
79	204.40	19.87	18.53	419.15	1667.90	1710.35	0.94	265.45
80	191.38	19.59	18.75	417.08	1447.16	1533.12	0.94	265.76
81	210.98	23.20	19.88	441.00	1625.68	1648.34	0.94	266.37
82	181.20	18.78	19.37	372.65	1472.29	1487.55	0.93	269.90
83	201.20	21.61	21.89	416.17	1564.85	1672.85	0.94	266.06
84	190.69	19.87	18.55	354.63	1513.34	1551.51	0.94	265.45
85	204.51	21.58	19.95	420.17	1671.91	1712.73	0.94	265.71
86	181.82	16.02	18.53	351.02	1551.00	1681.22	0.94	265.35
87	202.98	19.93	18.04	355.78	1434.18	1443.20	0.94	265.45
88	201.64	18.91	21.34	371.56	1434.72	1555.83	0.94	265.40
89	180.40	16.08	18.04	351.00	1443.20	1680.25	0.94	266.79
90	190.76	19.58	18.056	418.28	1447.28	1533.12	0.94	265.73
91	181.22	17.94	19.98	391.80	1493.28	1521.72	0.92	270.72
92	211.60	19.65	18.98	369.44	1472.21	1503.33	0.93	270.23
93	181.20	20.08	21.69	431.80	1533.20	1671.00	0.93	269.89
94	181.02	20.11	19.97	372.98	1504.03	1713.24	0.94	265.66
95	191.05	20.16	19.35	373.59	1504.03	1713.24	0.94	265.99
96	200.67	19.11	18.07	391.80	1557.08	1726.22	0.92	270.58
97	201.64	22.63	21.36	371.56	1592.69	1680.79	0.94	266.80
98	189.97	19.72	18.70	419.14	1447.16	1533.12	0.94	265.73
99	212.39	23.07	19.93	438.94	1625.68	1648.34	0.94	266.40
100	191.60	19.58	21.30	439.00	1447.16	1533.12	0.92	270.23
101	204.40	21.58	19.95	357.61	1671.91	1712.73	0.94	265.7
102	204.51	19.87	18.53	418.37	1551.00	1681.22	0.94	265.45
103	191.38	19.60	18.75	417.08	1447.16	1447.80	0.94	265.44
104	202.98	19.92	18.04	355.78	1434.18	1528.52	0.94	265.77
105	189.80	19.58	18.06	354.56	1433.92	1444.66	0.94	265.73
106	203.94	19.93	18.04	419.50	1447.51	1531.66	0.94	265.45
107	187.57	19.58	18.01	418.28	1447.25	1534.27	0.94	265.74
108	204.40	18.83	21.94	371.8	1563.70	1680.79	0.93	266.05
109	181.82	16.02	18.53	351.02	1551.00	1671.39	0.94	265.37
110	204.51	21.58	19.95	420.17	1681.73	1712.73	0.94	265.69
111	204.40	19.87	18.53	372.93	1447.03	1658.58	0.94	265.39
112	201.64	18.91	21.34	415.40	1555.83	1698.03	0.94	265.45

113	180.34	21.58	18.30	358.91	1440.96	1444.05	0.94	265.71
114	190.86	16.08	19.78	411.09	1503.18	1706.46	0.94	265.36
115	180.40	16.08	18.08	351.36	1435.50	1443.20	0.94	265.36
116	204.40	19.87	18.49	355.44	1549.67	1681.22	0.94	265.45
117	201.64	18.91	21.34	370.31	1433.21	1555.83	0.94	265.39
118	204.40	19.87	18.53	419.15	1667.90	1711.86	0.94	265.45
119	190.59	19.85	18.53	371.71	1667.90	1710.35	0.94	265.45
120	204.86	20.19	19.35	421.03	1504.03	1713.24	0.93	265.99
121	201.64	18.92	18.50	371.56	1434.72	1553.45	0.94	265.40
122	204.40	19.87	21.38	355.80	1550.99	1681.22	0.94	265.45
123	204.51	21.58	18.42	357.35	1553.98	1671.91	0.94	265.35
124	181.82	16.02	20.07	413.84	1681.22	1709.75	0.94	265.71
125	204.40	19.87	18.53	355.80	1551.00	1681.22	0.94	265.45
126	181.82	16.58	18.53	351.02	1550.99	1671.42	0.94	265.37
127	204.51	21.02	18.42	357.35	1553.98	1671.88	0.94	265.35
128	180.40	16.03	18.06	351.36	1435.50	1443.15	0.94	265.3
129	191.38	19.65	18.76	417.08	1447.16	1447.84	0.94	265.44
130	204.40	19.98	18.42	356.77	1667.83	1710.35	0.94	265.45
131	204.51	21.78	18.53	419.73	1553.98	1671.98	0.94	265.35
132	180.40	16.08	18.11	351.19	1434.18	1443.20	0.94	265.31
133	191.38	19.60	18.68	416.90	1447.16	1447.80	0.94	265.44
134	203.10	19.87	21.38	355.78	1447.52	1681.22	0.94	265.45
135	204.28	19.93	18.04	355.80	1443.20	1537.66	0.94	265.45
136	190.86	16.22	19.53	370.86	1439.29	1501.58	0.94	265.36
137	201.64	18.77	21.44	410.55	1557.42	1700.38	0.94	265.39
138	204.51	16.13	18.42	350.60	1553.98	1671.91	0.94	265.35
139	180.40	21.53	18.04	357.75	1434.18	1443.20	0.94	265.36
140	204.51	19.94	18.52	355.91	1553.97	1670.93	0.94	265.35
141	204.40	21.51	21.28	357.24	1550.99	1682.19	0.94	265.45
142	201.64	18.91	18.77	352.79	1433.21	1555.83	0.94	265.39
143	181.82	16.02	21.11	368.55	1550.99	1681.22	0.94	265.35
144	180.37	16.02	18.08	351.36	1435.50	1451.13	0.94	265.36
145	181.85	16.08	18.53	351.02	1551.00	1663.46	0.94	265.37
146	204.40	19.87	18.53	352.83	1447.03	1658.60	0.94	265.39
147	204.40	19.87	18.53	375.90	1551.00	1681.20	0.94	265.45
148	182.00	16.02	18.53	351.02	1551.00	1671.39	0.94	265.37
149	201.46	18.91	21.34	371.56	1434.72	1555.83	0.94	265.40
150	204.40	19.87	18.53	355.80	1551.00	1681.22	0.94	265.45